

# Mechanism of Gold-Catalyzed Carbon Material Growth

Daisuke Takagi,<sup>†</sup> Yoshihiro Kobayashi,<sup>‡,§</sup> Hiroki Hibino,<sup>‡</sup>  
Satoru Suzuki,<sup>‡</sup> and Yoshikazu Homma<sup>\*,†,§</sup>

Department of Physics, Tokyo University of Science, Shinjuku, Tokyo 162-8601, Japan,  
NTT Basic Research Laboratories, NTT Corporation, Atsugi,  
Kanagawa 243-0198, Japan, and CREST, Japan Science and Technology Agency,  
Chiyodaku, Tokyo 102-0075, Japan

Received November 6, 2007; Revised Manuscript Received January 6, 2008

## ABSTRACT

We demonstrate that nanosized Au particles have carbon solubility. Au-catalyzed carbon material growth by chemical vapor deposition undergoes a structural change, either a carbon nanowire or a single-walled carbon nanotube, depending on the catalyst particle size. This carbon material growth from Au is derived by the formation of Au–C eutectic nanosized alloy.

Nanosized iron-group metals (Fe, Co, and Ni) are known to catalyze single-walled carbon nanotube (SWCNT) growth in chemical vapor deposition (CVD).<sup>1</sup> For the precise structural control of SWCNTs such as the chirality, the mechanism of SWCNT growth from iron-group catalysts has been investigated by molecular dynamics calculations and experimental studies.<sup>2–6</sup>

A common understanding of the SWCNT growth processes from iron-group catalysts by CVD is that carbon-bearing molecules are catalytically decomposed on the catalyst surface, resulting in the incorporation of carbon atoms into the catalyst. Once supersaturation is formed, carbon atoms precipitate from the catalyst, which leads to nanotube growth. The vapor–liquid–solid (VLS) mechanism is one explanation of carbon uptake and supersaturation in the catalyst.<sup>7</sup> The VLS growth mechanism is based on the solubility of carbon in catalyst metals. However, it has recently been reported that even gold (Au) acts as a catalyst for SWCNT synthesis.<sup>8,9</sup> Unlike the iron-group elements, the carbon solubility of Au is extremely low in bulk phase.<sup>10</sup> For the clarification of the SWCNT growth mechanism from metal catalysts, it is necessary to consider the results of Au-catalyzed SWCNT growth.

The catalysis of Au for SWCNT growth depends on the catalyst particle size: SWCNTs can be synthesized from Au particles 5 nm or smaller in diameter.<sup>8</sup> The question is: What is the mechanism of SWCNT growth from Au nanoparticles. In the present study, we investigated the Au-catalyzed

SWCNT growth mechanism using site- and size-controlled Au nanoparticles on atomic steps of a Si surface.

The size of Au nanoparticles could be controlled by the amount of Au deposited and the step spacing of the Si substrate during *in situ* observation by low-energy electron microscopy (LEEM).<sup>11</sup> In this method, obtained nanoparticles are Au–Si alloy not pure Au. Since the concentration of Au in Au–Si eutectic alloy is about 80 atom %,<sup>12</sup> Au–Si is expected to behave similarly to Au. (This similarity between Au–Si and Au is described later.) This means that the results of SWCNT growth from Au–Si nanoparticles would be applicable to the discussion of the Au-catalyzed SWCNT growth mechanism.

In the present study, both Au–Si and pure Au nanoparticles were employed as catalysts for carbon material growth. Pure Au particles were prepared by conventional vacuum deposition. All carbon materials were synthesized by CVD. The carbon material growth source was ethanol (850 °C growth temperature) or methane (1100 °C growth temperature). Details about the Au–Si nanoparticle formation and CVD condition for carbon material synthesis are described in the Supporting Information. Here, we should note that the Au-nanoparticle-deposited Si substrates were heated in air up to 850 °C. Thus, the Si surfaces were oxidized.

First, we show the results for about 10–30 nm Au–Si nanoparticles, which were obtained using a Si(111) substrate with a step spacing of about 500 nm. A LEEM image of self-assembled Au–Si nanoparticles on atomic steps of Si surface is shown in Figure 1a, where the white and the black arrows indicate an Au–Si nanoparticle and an atomic step, respectively. The atomic force microscope (AFM) image of Au–Si nanoparticles in Figure 1b reveals that the

\* Corresponding author. E-mail: homma@rs.kagu.tus.ac.jp.

† Department of Physics, Tokyo University of Science.

‡ NTT Basic Research Laboratories, NTT Corp.

§ CREST, Japan Science and Technology Agency.

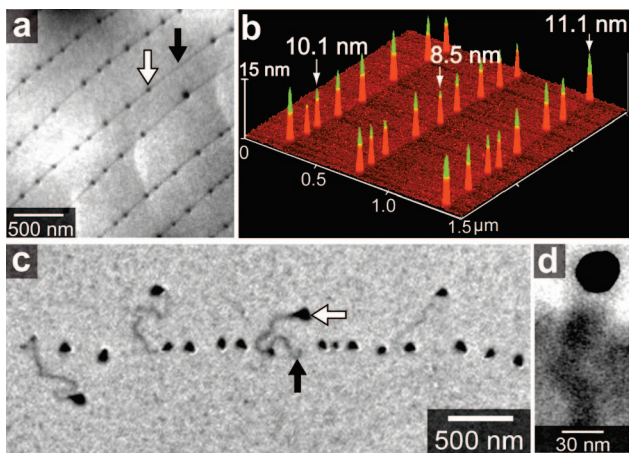


**Figure 1.** CNW growth from site- and size-controlled Au–Si nanoparticles. (a) LEEM image of Au–Si nanoparticles on atomic steps on a Si surface. (b) AFM image of Au–Si nanoparticles (10 nm mean diameter) on atomic steps. The step spacing is 500 nm. (c) SEM image of CNW growth from Au nanoparticles (30 nm mean diameter), in which white and black arrows indicate the Au–Si catalyst that has moved from the atomic step and original position of the Au–Si catalyst, respectively. (d) TEM image of grown CNW.

height of nanoparticles is about  $10 \pm 2$  nm. Au–Si particle size is controlled by the amount of Au deposited. We investigated the carbon material growth from the 10–30 nm Au–Si nanoparticles. Figure 1c is a scanning electron microscope (SEM) image of the sample surface after ethanol CVD. This SEM image indicates that Au–Si nanoparticles have the catalysis for the wirelike material synthesis. Since the source molecules were ethanol, the wirelike structure should be composed of carbon. The transmission electron microscope (TEM) image in Figure 1d shows that grown structures are amorphous carbon nanowires (CNWs). From the results of Figure 1, it is clear that Au–Si nanoparticles of 10–30 nm act as catalysts for CNW growth.

Aligned Au–Si nanoparticles on atomic steps are useful for characterizing the growth behavior of the product material from the catalyst. As shown in Figure 1c, inactive Au–Si nanoparticles remained at the original position along the atomic step. On the other hand, active Au–Si nanoparticles moved from their original position after CVD and stayed at one end of the CNW. The other end of the CNW is located at the atomic step. All active catalysts showed the same behavior.

To investigate the carbon material growth from small Au–Si nanoparticles, we prepared Au–Si nanoparticles using a Si(111) substrate with bunched atomic steps and a narrow terrace spacing of about 150 nm. The AFM image in Figure 2a proves that Au–Si nanoparticles of  $4 \pm 1.5$  nm aligned along the bunched atomic steps. The SEM images after the ethanol CVD are shown in Figure 2b. Grown materials, nanosize Au particles, and atomic steps can be imaged by SEM,<sup>13,14</sup> in which black wirelike and white wirelike contrasts are grown carbon materials that lie on the substrate surface and float above it, respectively. TEM observation and Raman scattering indicate that the grown materials are SWCNTs not CNWs. The TEM image in

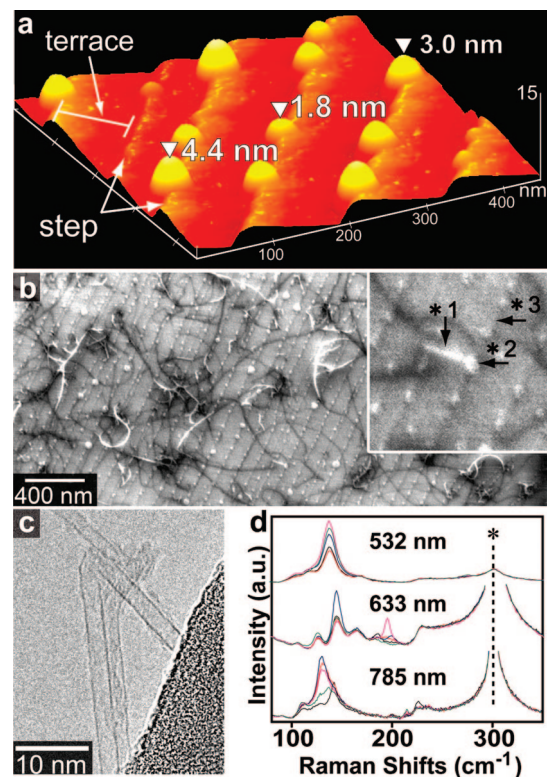


**Figure 2.** SWCNT growth from site- and size-controlled Au–Si nanoparticles. (a) AFM image of Au–Si nanoparticles (5 nm or smaller in size) on bunched atomic steps on Si surface. The step spacing is 150 nm. (b) SEM image of CNW growth from Au nanoparticles (inset: magnified image). (c) TEM image of grown SWCNTs. (d) Raman spectra of grown SWCNTs. The asterisk shows the silicon-originated signals.

Figure 2c confirms that the synthesized carbon material from Au–Si has a tubular structure of a single layer. Raman spectra obtained with excitation wavelengths of 532, 633, and 785 nm are shown in Figure 2d. Signals originating from the vibration of the radial direction of SWCNTs (called radial breathing mode, RBM) are observed clearly in the low-frequency region of the Raman spectra. The SWCNT diameters can be estimated to 1.0–1.8 nm from the Raman shift of the RBM peaks.<sup>15,16</sup> In the inset of Figure 2b (magnified image), we can clearly observe SWCNT (\*1) grown on an Au–Si nanoparticle (\*2) on a bunched atomic step (\*3). This SEM image reveals that almost all of the SWCNTs grow from particles fixed to steps.

We demonstrated that Au–Si nanoparticles produce, depending on their size, either CNWs or SWCNTs and that the critical catalyst diameter separating CNWs and SWCNTs is around 5 nm. Au is the major component of Au–Si alloy. Therefore, Au may play a dominant role as a catalyst of carbon material growth, and pure Au should also lead to the size-dependent structural change of Au-catalyzed carbon materials, just like Au–Si nanoparticles did. We examined CVD growth using pure Au particles  $10 \pm 1.5$  nm in size on  $\text{SiO}_2$  and aluminum hydroxide ( $\text{AlOOH}$ ) substrates. TEM images of vertical CNW growth from pure Au nanoparticles are shown in Figures 3a and 3b for methane CVD, and in Figure 3c for ethanol CVD. Each CNW has a Au nanoparticle on the top. The results of an energy dispersive X-ray

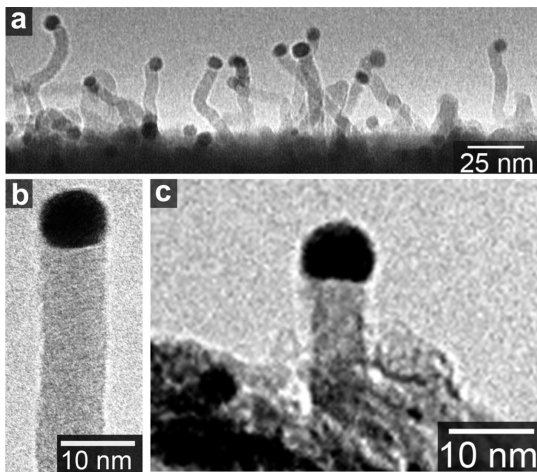


**Figure 3.** CNW growth from Au nanoparticles. (a) CNW growth on  $\text{SiO}_2$  substrate in methane ambient at  $1100\text{ }^\circ\text{C}$ . (b) Magnified CNW image from substrate of (a). (c) CNW growth on  $\text{AlOOH}$  substrate in ethanol ambient at  $850\text{ }^\circ\text{C}$ .

analysis of the Au nanoparticle on the CNW in Figure 3c are shown in Figure S1. Although the growth temperatures were different between the methane CVD ( $1100\text{ }^\circ\text{C}$ ) and ethanol CVD ( $850\text{ }^\circ\text{C}$ ), the grown materials were both amorphous nanowires and the Au particles showed hemispherical shapes, indicating they were molten during CVD.

The above results show that pure Au nanoparticles can also produce, depending on their size, either SWCNTs<sup>8</sup> or CNWs. From the results in Figures 1–3, we can conclude that (i) unlike bulk Au, nanosized Au has carbon solubility, and that (ii) Au forms Au–C nanoalloy droplets (liquid phase) and produces a CNW by the VLS mechanism. These conclusions can be deduced from the similarity of the Au-catalyzed semiconductor nanowire growth.<sup>17</sup> During Au-catalyzed silicon nanowire (SiNW) growth, the Au particle incorporates Si atoms and forms the Au–Si eutectic alloy.<sup>18</sup> Au-catalyzed VLS-like CNW growth means that carbon is soluble in a nanosized Au particle and forms Au–C eutectic alloy, just like in the SiNW growth from Au catalyst. Since no eutectic phase with carbon has been observed for bulk Au, these phenomena are a feature specific to a nanosize Au particle.

These phenomena provide insights into the mechanism of carbon material growth from Au catalysts. When Au catalyst particle size is large ( $10\text{--}30\text{ nm}$ ), CNWs are grown. The VLS mechanism reasonably explains the CNW formation. Au nanoparticles probably form a eutectic alloy with carbon and are present in a liquid phase (droplet) in the carbon material growth ambient. Au droplets have a high surface tension, as indicated by their spherical shape. On the other hand, when a carbon layer is formed, it lowers the interface energy between Au droplets and the substrate. Therefore, super-saturated carbon atoms precipitate at the Au droplet–substrate interface, and this brings the CNW formation.

When the catalyst size becomes small, SWCNTs are grown from Au catalysts instead of CNWs. This structural change from CNW to SWCNT is caused by an increase of carbon solubility in Au and the critical energy of nanowire nucleation. The size dependence of the solubility in Au is shown

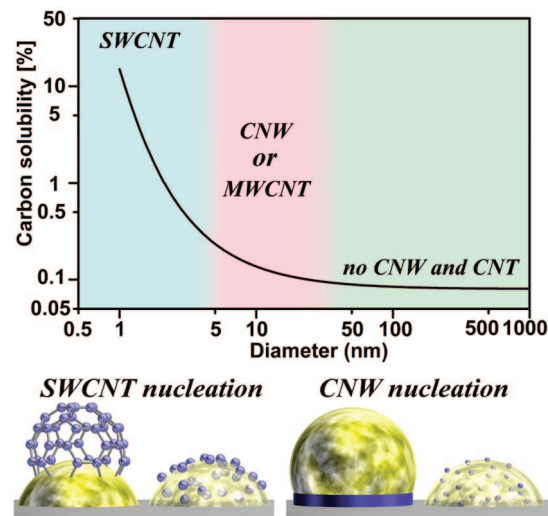


**Figure 4.** Carbon solubility in Au from the bulk phase to nanosized particle and structural change of Au-catalyzed carbon materials. Carbon solubility is indicated in molar fraction in this figure, instead of molality in eq 1.

in Figure 4. The solubility  $S$  in the particle with radius  $r$  is estimated as<sup>19</sup>

$$S = S_0 \exp(2\sigma V/kTr) \quad (1)$$

where  $S_0$  is the solubility in bulk material, defined as the ratio of the amounts of solute and solvent,  $\sigma$  is the surface tension,  $V$  is the volume of a metal molecule,  $k$  is the Boltzmann constant, and  $T$  is the melting temperature in bulk phase. For  $\sigma$  and  $S_0$ , the values in refs 20 and 10 were used. The carbon solubility in bulk Au is extremely low.<sup>10</sup> However, in small Au particles ( $5\text{ nm}$  or smaller), the carbon solubility should increase drastically. With the increase of carbon solubility in Au, the driving force of carbon precipitation from Au is suppressed. Additionally, the decrease of particle size leads to increase of the critical energy of nanowire nucleation from the catalyst particle, which has been shown by thermodynamics calculation and experimental studies for SiNWs.<sup>21–23</sup> By these phenomena, the CNW nucleation from a small Au catalyst particle is suppressed. Furthermore, in small size Au particle, carbon may preferentially precipitate on the Au particle surface because the surface tension of graphite is smaller than that of Au.<sup>20,24</sup> Consequently, carbon atoms not used for the CNW synthesis form a carbon network on the Au particle surface as the nucleus of the SWCNT cap, and this cap nucleation derives the SWCNT formation.<sup>25</sup> The Au particle size determines the upper bound of SWCNT diameter, and SWCNTs thinner than the Au particle size can be grown.<sup>14</sup>

In the present study, Au (Au–Si) nanoparticles of  $10\text{--}30\text{ nm}$  produced CNWs. On the other hand, growth of multi-walled CNTs (MWCNTs) has been reported from Au nanoparticles in this size range when they were supported on  $\text{Al}_2\text{O}_3$  and  $\text{C}_2\text{H}_2$  was used as the carbon source.<sup>26</sup> The carbon precipitation mechanism in the MWCNT case might be similar to that for CNWs described above. Carbon atoms in a nanoparticle precipitate at the interface between the nanoparticle and the substrate when the particle size is  $10\text{--}30\text{ nm}$  and form either a CNW or a MWCNT. The factor that determines whether a CNW or MWCNT is formed is not clear, but it could be the interface energy or the precipitation

rate of carbon atoms on the interface of Au catalyst particle and the substrate. We believe the model of structural change from CNW to SWCNT depending on catalyst particle size can be applied to the iron-group and other conventional catalyst metals. In these cases, MWCNTs are preferentially grown instead of CNW probably because of their catalytic function of graphitization.

Iron-group metals have high carbon solubility in the bulk phase.<sup>19</sup> Because of this high carbon solubility, iron-group metals can produce carbon materials from large particles. However, since Au does not have carbon solubility in the bulk phase, carbon materials cannot be produced from large particles. When Au particle size becomes several tens of nanometers, it has carbon solubility as shown in Figure 4. As a result, carbon materials are produced from Au catalyst particles. This model of carbon solubility in nanosized particles would be valid for other catalysts. For instance, recently, it has been reported that small germanium particles act as catalysts for SWCNT growth,<sup>25</sup> though germanium has little solubility for carbon in the bulk phase. We should note that the present model is based on the VLS picture and explains the catalyst size dependence of carbon uptake/precipitation. Recently, Kodambaka et al. reported that Ge nanowires grew in a similar way to VLS from solid Au—Ge at below the Au—Ge eutectic point.<sup>27</sup> In the present study, the growth temperatures were higher than the melting points of nanosized Au,<sup>28</sup> but taking a liquid phase might not be essential for a high carbon solubility in nanoparticles.

**Supporting Information Available:** Description of experimental methods and figure of high-resolution TEM and EDX spectrum of Au-catalyzed CNW on Al hydroxide substrate. This material is available free of charge via Internet at <http://pubs.acs.org>.

## References

- Kong, J.; Cassell, A. M.; Dai, H. *Chem. Phys. Lett.* **1998**, *292*, 567–574.
- Shibuta, Y.; Maruyama, S. *Chem. Phys. Lett.* **2003**, *382*, 381–386.
- Ding, F.; Bolton, K. *Nanotechnology* **2006**, *17*, 543–548.
- Bladh, K.; Falk, L. K. L.; Rohmund, F. *Appl. Phys. A: Mater. Sci. Process.* **2000**, *70*, 317–322.
- Li, Y. M.; Kim, W.; Zhang, Y. G.; Rolandi, M.; Wang, D. W.; Dai, H. *J. Phys. Chem. B* **2001**, *105*, 11424–11431.
- Harutyunyan, A. R.; Mora, E.; Tokune, T.; Bolton, K.; Rosen, A.; Jiang, A.; Awasthi, N.; Curtarolo, S. *Appl. Phys. Lett.* **2007**, *90*, 163120–1163120–3.
- Gavillet, J.; Loiseau, A.; Journet, C.; Willaime, F.; Ducastelle, F.; Charlier, J. C. *Phys. Rev. Lett.* **2001**, *87*, 275504–1–275504–4.
- Takagi, D.; Homma, Y.; Hibino, H.; Suzuki, S.; Kobayashi, Y. *Nano Lett.* **2006**, *6*, 2642–2645.
- Bhaviripudi, S.; Mile, E.; Steiner, S. A.; Zare, A. T.; Dresselhaus, M. S.; Belcher, A. M.; Kong, J. *J. Am. Chem. Soc.* **2007**, *129*, 1516–1517.
- Okamoto, H.; Massalski, T. B. *Bull. Alloy Phase Diagrams* **1984**, *5*, 378–379.
- Hibino, H.; Watanabe, Y. *Surf. Sci.* **2005**, *588*, L233–L238.
- Binary Phase Diagrams*; Massalski, T. B., Ed.; American Society of Metals: Metals Park, OH, 1986.
- Homma, Y.; Tomita, M.; Hayashi, T. *Surf. Sci.* **1991**, *258*, 147–152.
- Takagi, D.; Yamazaki, A.; Otsuka, Y.; Yoshimura, H.; Kobayashi, Y.; Homma, Y. *Chem. Phys. Lett.* **2007**, *445*, 213–216.
- Rao, A. M.; Richter, E.; Bandow, S.; Chase, B.; Eklund, P. C.; Williams, K. A.; Fang, S.; Subbaswamy, K. R.; Menon, M.; Thess, A.; Smalley, R. E.; Dresselhaus, G.; Dresselhaus, M. S. *Science* **1997**, *275*, 187–191.
- Kataura, H.; Kumazawa, Y.; Maniwa, Y.; Umezawa, I.; Suzuki, S.; Ohtsuka, Y.; Achiba, Y. *Synth. Met.* **1999**, *103*, 2555–2558.
- Duan, X. F.; Lieber, C. M. *Adv. Mater.* **2000**, *12*, 298–302.
- Wagner, R. S.; Ellis, W. C. *Appl. Phys. Lett.* **1964**, *4*, 89–90.
- Moisala, A.; Nasibulin, A. G.; Kauppinen, E. I. *J. Phys.: Condens. Matter* **2003**, *15*, S3011–S3035.
- Sambles, J. R. *Proc. R. Soc. London, Ser A* **1971**, *324*, 339–351.
- Wang, C. X.; Wang, B.; Yang, Y. H.; Yang, G. W. *J. Phys. Chem. B* **2005**, *109*, 9966–9969.
- Wu, Y.; Cui, Y.; Huynh, L.; Barrelet, C. J.; Bell, D. C.; Lieber, C. M. *Nano Lett.* **2004**, *4*, 433–436.
- Schmidt, V.; Senz, S.; Gosele, U. *Nano Lett.* **2005**, *5*, 931–935.
- Jakubov, T. S.; Mainwaring, D. E. *J. Colloid Interface Sci.* **2007**, *307*, 477–480.
- Takagi, D.; Hibino, H.; Suzuki, S.; Kobayashi, Y.; Homma, Y. *Nano Lett.* **2007**, *7*, 2272–2275.
- Lee, S. Y.; Yamada, M.; Miyake, M. *Carbon* **2005**, *43*, 2654–2663.
- Kodambaka, S.; Tersoff, J.; Reuter, M. C.; Ross, F. M. *Science* **2007**, *316*, 729–732.
- Buffat, Ph.; Borel, J.-P. *Phys. Rev. A* **1976**, *13*, 2287–2298.

NL0728930